

Noncovalent Immobilization of a Nickel Cyclam Catalyst on Carbon Electrodes for CO₂ Reduction Using Aqueous Electrolyte

Francesca Greenwell, Gaia Neri, Verity Piercy and Alexander J. Cowan*

Department of Chemistry and Stephenson Institute for Renewable Energy, University of Liverpool, Liverpool UK

acowan@liverpool.ac.uk

Abstract A pyrene modified nickel cyclam catalyst ($[\text{Ni}(\text{CycPy})]^{2+} = \text{Ni}(1-(4-(\text{pyren-1-yl)butyl})-1,4,8,11\text{-tetraazacyclotetradecane})$) has been synthesised and electrochemically characterised under both CO₂ and N₂. The pyrene functional group forms a non-covalent interaction with carbon electrode supports and the immobilised $[\text{Ni}(\text{CycPy})]^{2+}$ complex remains electroactive. We report a $[\text{Ni}(\text{CycPy})]^{2+}$ modified gas diffusion electrode (GDE) that is tested in aqueous electrolyte and shown to be active towards CO production. This is the first successful demonstration of a nickel cyclam modified GDE in aqueous solvent and shows the potential of this class of catalysts for use in co-electrolysis devices.

1. Introduction

The renewable utilisation of CO₂ as a chemical feedstock for fuel production has driven the development of selective electrocatalysts over the past 40 years. The reduction of CO₂ and water to syngas is a frequently targeted reaction due to the variety of hydrocarbon products available through the well-established Fisher-Tropsch process.¹⁻³ Various electrochemically generated oxidation states of metal complexes have been proposed for CO₂-to-CO conversion, with molecular complexes offering tunability of the overpotentials and selectivity.⁴ However, more recently it has been established that to use these electrocatalysts practically, immobilisation to the working electrode is extremely advantageous, thus harnessing the selectivity of well-defined molecular catalysts while overcoming problems such as poor solubility, low activity and recyclability.⁵

Nickel cyclams (cyclam (Cyc) = 1,4,8,11-tetraazacyclotetradecane) are a class of low-cost, well studied electrocatalysts for CO₂ reduction, showing high selectivity for CO in aqueous electrolyte.⁶⁻⁹ Their mechanism has been studied extensively and the key steps proposed are; initial reduction of [Ni(Cyc)]²⁺ to [Ni(Cyc)]⁺ which is accompanied by CO₂ binding to form a Ni^I-CO₂ adduct,^{10,11} the adduct can then undergo protonation, although this may occur during CO₂ binding,¹² then further reduction (with protonation) to yield water and a Ni^{II}-CO species is thought to occur from which the CO can be released. The exact mechanism of the protonations and electron transfer remains experimentally unproven but recent DFT calculations indicate concerted proton-electron transfer and C-O bond cleavage is the lowest energy pathway.^{9,11,13,14} [Ni(Cyc)]²⁺ has been most frequently studied on Hg electrodes, originally due to the extensive solvent window of the Hg electrode in aqueous media.^{7,9} However, it was quickly established that the catalyst underwent reductive adsorption on the Hg electrode surface to give the catalytically active adsorbed [Ni(Cyc)]⁺ species¹⁵⁻¹⁷ which aided electrochemical CO₂ reduction. The mechanism of surface-enhancement on Hg may be in part

explained by repression of the catalyst degradation pathway or it may be due to a preferential formation of the catalytically active conformational isomer.¹⁸ $[\text{Ni}(\text{cyc})]^{2+}$ has 5 conformational isomers in solution,¹⁹ but 2 of these (Trans I and III) account for >99% of molecules.¹⁹ DFT calculations initially suggested that on mercury electrodes rearrangement preferentially forms the Trans-I isomer occurs and that this is the catalytically active species,²⁰ but a subsequent study has since proposed that the Trans-III isomer is adsorbed and that it flattens to become the active catalyst.¹⁸

While $[\text{Ni}(\text{Cyc})]^{2+}$ is most active on mercury electrodes, the complex is also active for CO_2 reduction at non-toxic metals^{18,21} and when used as homogenous electrocatalyst with glassy carbon (GCE) electrodes.²² Incorporating $[\text{Ni}(\text{Cyc})]^{2+}$ onto a low cost, non-toxic electrode surface, such as a carbon felt, has since been of great interest as a route to developing practical electrode structures, for example a gas diffusion electrode for use in a CO_2 /water co-electrolysis device.^{17,23–25} Kubiak and co-workers modified a GCE with a series of $[\text{Ni}(\text{alkynyl-cyclam})]^{2+}$ catalysts using direct anodic electrografting; there, a positive shift in the reduction potential of *ca.* 0.2 V compared with the homogeneous system was observed.²⁶ Once grafted bulk electrolysis studies showed that the catalysts produced primarily H_2 , with only low levels of CO produced in a mixed $\text{CH}_3\text{CN}/\text{H}_2\text{O}$ (5:1 vol.) solvent. One possible reason for the low selectivity towards CO_2 was the effect of functionalisation of one of the cyclam N-H groups, which is known to decrease selectivity.^{14,16,22} However cyclic voltammetry (CV) studies showed that the complexes had a good reactivity towards CO_2 when used as a solution catalyst in the same electrolyte at a carbon electrode. Alternatively, it is possible that immobilisation onto the electrode surface led to constraints upon the cyclam structure at the electrode surface, reducing its ability to selectively reduce CO_2 .

An alternative route to functionalise carbon electrodes is to exploit the sp^2 carbon structure and use non-covalent π - π interactions to adhere a complex to the surface, for example through the

use of a pyrene unit. Modifying CO₂ reduction catalysts with a pyrene group was reported by Blakemore *et al.* who synthesised a Re complex bearing two pyrene functionalities before mixing the complex with carbon black and depositing it onto highly oriented pyrolytic graphite.²⁷ Kang and co-workers were able to reduce CO₂ to formate with high TONs (54000) with a pyrene modified iridium pincer catalyst on carbon nanotubes (CNTs).²⁸ An iron-porphyrin was successfully modified with a pyrene group and immobilised onto CNTs by Robert and co-workers.²⁹ Reuillard *et al.* also used a pyrene modification on a Mn(bipyridine) complex to non-covalently attach the CO₂ reduction catalyst to a CNT electrode.³⁰ The latter three examples remain among the few molecular catalysts to show high catalytic activity after immobilization while working in aqueous conditions. Recently the first pyrene modified Ni cyclam catalyst was reported by Fontecave *et al* and shown to be immobilised onto CNTs drop-casted on a gas diffusion layer. The immobilised catalyst showed a high TON and a FE of 90% for CO and 10% for H₂ in CH₃CN with 1% water.³¹

The achievement of a CO₂ selective Ni cyclam catalyst immobilised onto a carbon support is an important step forwards for the field but this was achieved in aprotic solvent with a very low (1%) water content, conditions which will suppress competitive H₂ evolution. In solution there are multiple reports of good levels of selectivity towards CO₂ for [Ni(cyclam)]²⁺ complexes when used with a glassy carbon electrode and on a mercury electrode but its activity when immobilised on a carbon electrode in an aqueous solvent remains unproven.^{10,21–23} If this class of catalysts is to be applied in CO₂/water co-electrolysis devices it is important to understand if following surface immobilisation the catalyst can retain its selectivity towards CO₂ reduction in water. Here we report an alternative pyrene functionalised nickel cyclam, Ni(1-(4-(pyren-1-yl)butyl)-1,4,8,11-tetraazacyclotetradecane, labelled hereafter, [Ni(CycPy)]²⁺. We examine the electrochemical behaviour of the complex both in solution and following successful immobilisation, onto a carbon electrode. Finally, we report its activity on

a gas diffusion electrode (GDE) support in 0.5 M KHCO_3 and for the first time show that the catalyst is active towards CO_2 reduction when immobilised in an aqueous gas diffusion electrolyser.

2. Experimental

All chemicals and solvents were purchased from Sigma Aldrich and used without further purification, aside from acetonitrile and tetrabutylammonium hexafluorophosphate used in the electrochemical measurements. CH_3CN was stored under activated molecular sieves to remove trace water; TBAPF_6 was purified by hot recrystallization from ethanol, followed by drying in vacuo and was stored under an inert atmosphere. $>99.5\%$ KHCO_3 was used as received. Milli-Q water ($18.2 \text{ M}\Omega$) was used throughout. Ar, N_2 and CO_2 and CO_2/CH_4 (1%) were purchased from BOC at CP or higher grade. The gas diffusion layer (GDL) ELAT LT1400 was purchased from Fuel Cell Store. The Selemion AMV-N membrane was purchased from Bellex International Corporation.

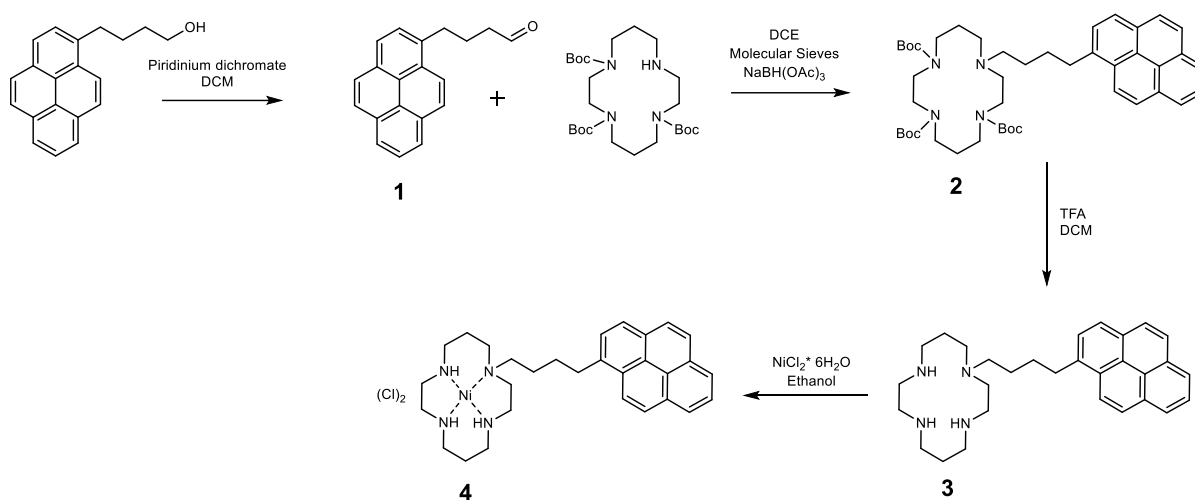
Characterization ESI-MS and elemental analyses were performed by the University of Liverpool analytical services. ^1H and ^{13}C NMR spectra were recorded on a Bruker 400 MHz spectrometer.

Synthesis. 1-(4-(pyren-1-yl)butyl)-1,4,8,11-tetraazacyclotetradecane (CycPy) was prepared using a previously described method, full details can be found in the supporting information.³² For the synthesis of Ni(1-(4-(pyren-1-yl)butyl)-1,4,8,11-tetraazacyclotetradecane)dichloride ($\text{Ni}(\text{cycPy})\text{Cl}_2$), a solution of CycPy (47 mg, 0.1 mmol) in ethanol (5 ml) at room temperature and a solution of $\text{NiCl}_2 \cdot 6\text{H}_2\text{O}$ (24 mg, 0.1 mmol) in ethanol (5ml) were added. The mixture turned bright orange upon contact. The solution was left at room temperature for 48h. After which, purple crystals had formed, and the intensity of the colour of the solution had dropped

significantly. The purple crystals were filtered and washed three times with ethanol and left to dry in air. Obtained: 38.20 mg, yield: 54%. UV-vis (MeOH): $\lambda_{\text{max}} = 463$ nm. MS (ESI+): m/z calcd. For $\text{C}_{30}\text{H}_{40}\text{Cl}_2\text{N}_4\text{Ni}$: 586.27, found: 549.2 $[\text{M}-\text{Cl}]^+$ CHN microanalysis: anal. calcd. for $\text{C}_{30}\text{H}_{40}\text{Cl}_2\text{N}_4\text{Ni}$: C, 61.46, H, 6.88, N, 9.56; found: C, 61.65, H, 6.73, N, 9.41.

Electrochemistry Electrochemical experiments were carried out using a PalmSens3 potentiostat (Alvatek) or a biologic SP-200 potentiostat. Solution experiments used a glassy carbon electrode (BASi) as the working electrode, a platinum mesh as the counter electrode, and a Ag/AgCl reference electrode. In mixed solvents the stability of the reference electrode was assessed by comparison to the reported values of the ferrocene/ferrocenium redox couple in CH_3CN . The electrolyte was purged with either N_2 or CO_2 for 30 minutes before each experiment. 1cm^2 glassy carbon plates (BASi) were soaked in 1 mM solution of $[\text{Ni}(\text{CycPy})]^{2+}$ in methanol for 72h. The carbon plates were then washed with methanol followed by distilled water for the GCE/ $[\text{Ni}(\text{CycPy})]$ studies. A gas diffusion electrode (GDE) was prepared by spray coating down a catalyst ink (10.5 mg of $[\text{Ni}(\text{cycPy})]$, 8 mL methanol, 8 μL Nafion 117 (5 wt%) and 8 μL PTFE (60 wt%)) onto a 10.5 cm^2 area of ELAT LT1400. The anode was prepared by spray coating a catalyst ink (32 mg RuO_2 , 1 mL water and 1 mL propan-2-ol and 160 μL of Nafion 117 (5 wt%)) onto a 10.5 cm^2 area on a Ti plate. GDE electrochemical experiments were conducted in a commercial 4-compartment 10.5 cm^2 GDE flow cell (Electrocell Micro Flow cell), in a gas push through configuration. The electrolyte, 0.5 M KHCO_3 solutions were circulated at a rate of 22 mL min^{-1} and 12 mL min^{-1} , for the anolyte and catholyte, respectively. A leak-free Ag/AgCl (Alvatek) was used as a reference electrode (Alvatek) with GDE cathode and RuO/Ti plate anode. The anode and cathode were separated by a Selemion AMV-N membrane (Bellex). The flow of CO_2 was controlled by a Bürkert Type 8741 mass flow controller and was provided to the cell at a flow of 20 mL min^{-1} . The chronoamperometry measurement was run at -1.4 V vs Ag/AgCl for 2.5 hours. Bulk

electrolysis experiments used a CO₂ supply with 1% CH₄ added as an internal calibrant. Gas concentrations were measured by taking 500 μL injections of the cell headspace or the exhaust feed from the gas diffusion electrode and analysed using an Agilent 6890N with a 5 Å molecular sieve column (ValcoPLOT, 30 m length, 0.53 mm ID) and a pulsed discharge detector (D-3-I-HP, Valco Vici).



Scheme 1 Synthetic pathway to form [Ni(CycPy)]²⁺

Results and Discussion

The synthesis of the CycPy ligand has been previously reported but [Ni(CycPy)]²⁺ has not.³² The Synthesis is described in detail in the ESI and summarised in Scheme 1. The ¹H and ¹³C NMR spectra and the ESI mass spectrometry analysis of the CycPy ligand agree with the desired structure and past reports. The CHN elemental analysis suggests the presence of ammonium hydroxide as an impurity; this results from interaction of the ligand with the NH₄⁺ termination of the Amberlite resin used for the last purification steps. Further removal of the

ammonium hydroxide was not attempted as this was considered potentially beneficial for the Ni insertion reaction; we have previously noticed^{21,23} that an alkaline environment favours complexation due to the deprotonation of the macrocycle amines. Synthesis of the $[\text{Ni}(\text{CycPy})]^{2+}$ complex was attempted using various reaction conditions and solvents. To obtain the pure product both the ligand and nickel chloride hexahydrate were dissolved in ethanol prior to mixing. Over time as the complex formed it crashed out of ethanol as purple crystals with mass spectroscopy and elemental analysis confirming the successful synthesis of $[\text{Ni}(\text{CycPy})]^{2+}$. UV/Vis spectroscopy indicates that in water, methanol and a solvent mix of CH_3CN with 10% H_2O , $[\text{Ni}(\text{CycPy})]^{2+}$ exists primarily in the low spin, square planar form with minimal contribution from the distorted octahedral form with either solvent or chloride in the axial positions (figure S1). In DCM UV/Vis spectroscopy shows the complex preferentially forms the 6-coordinate octahedral species.²³

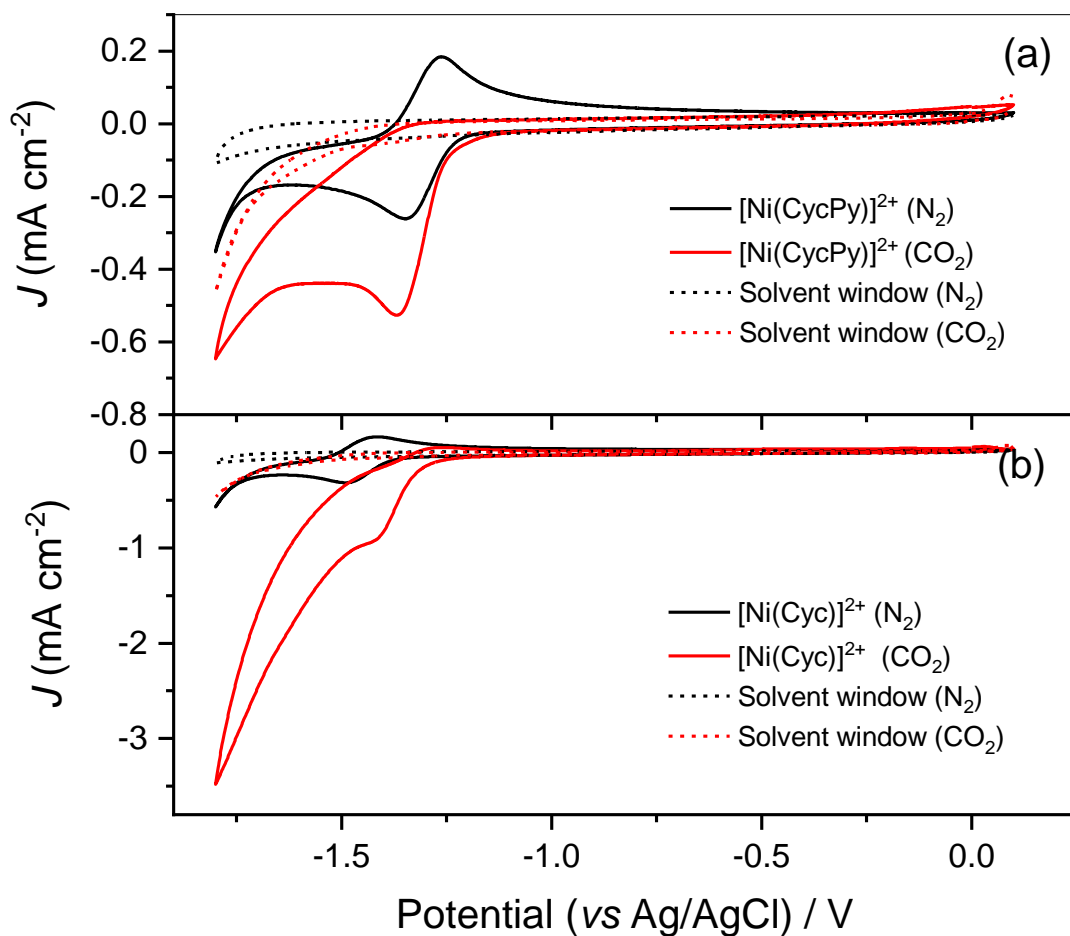


Figure 1 CVs of 1mM $[\text{Ni}(\text{CycPy})]^{2+}$ (top) and $[\text{Ni}(\text{Cyc})]^{2+}$ (bottom) in 0.1M TBA PF₆ CH₃CN with 10% water using a GCE; 100mV/s under N₂ (black) and CO₂ (red). The solvent window recorded under the same conditions in the absence of the catalysts is shown with dashed lines.

Electrochemical studies of $[\text{Ni}(\text{CycPy})]^{2+}$ in solution were carried out to examine the effect of addition of the pyrene group through alkylating one of the N atoms in the cyclam ring. CVs were recorded in 1 mM solutions of catalyst in CH₃CN with 10% water using a glassy carbon electrode as the working electrode, figure 1a. The complex is not fully soluble in CH₃CN in the absence of water. We also present the electrochemistry of an unmodified $[\text{Ni}(\text{Cyc})]^{2+}$

complex under the same conditions, figure 1b. The CVs under nitrogen show a redox couple at $-1.31 \text{ V}_{\text{Ag}/\text{AgCl}}$ which can be assigned to the $\text{Ni}^{\text{II/I}}$ reduction through comparison to the CV of $[\text{Ni}(\text{Cyc})]^{2+}$ ($-1.44 \text{ V}_{\text{Ag}/\text{AgCl}}$) and to literature.^{17,22,23} Variable scan rate CVs (figure S2-S4) show that the $\text{Ni}^{\text{II/I}}$ couple of $[\text{Ni}(\text{cycPy})]^{2+}$ is reversible under N_2 and that the response is dominated by freely diffusing species in solution. Any immobilised catalyst on the glassy carbon electrode provides a minimal contribution to the electrochemical response observed in figure 1. The $\text{Ni}^{\text{II/I}}$ couple of $[\text{Ni}(\text{CycPy})]^{2+}$ is *ca.* 150 mV more positive than the parent complex as a result of alkylating one of the N atoms in the cyclam ring, in-line with past studies which show similar positive shifts in the couple following substitution.^{16,22} Under CO_2 , the $\text{Ni}^{\text{II/I}}$ reduction becomes irreversible and an increase in current density is measured demonstrating that CO_2 catalysis is occurring. Comparison of the peak current density under catalytic conditions (j_c), and in the absence of the substrate (j_p), provides a comparative measure of catalytic activity. $j_c / j_p = 1.7$ for $[\text{Ni}(\text{CycPy})]^{2+}$ and 3.1 for $[\text{Ni}(\text{Cyc})]^{2+}$. Although the parent complex shows a larger catalytic current enhancement under CO_2 , the pyrene-modified cyclam has an electrocatalytic onset *ca.* 50 mV positive. Overall the CV analysis shows that in $\text{CH}_3\text{CN}/\text{H}_2\text{O}$ solution the electrochemical behaviour of the $[\text{Ni}(\text{CycPy})]^{2+}$ complex is similar to that of the parent $[\text{Ni}(\text{Cyc})]^{2+}$ complex with a slight decrease in catalytic activity, as would be anticipated from past studies which show that the binding constant of CO_2 decreases upon modification of the N-H groups of cyclam.^{11,17,33}

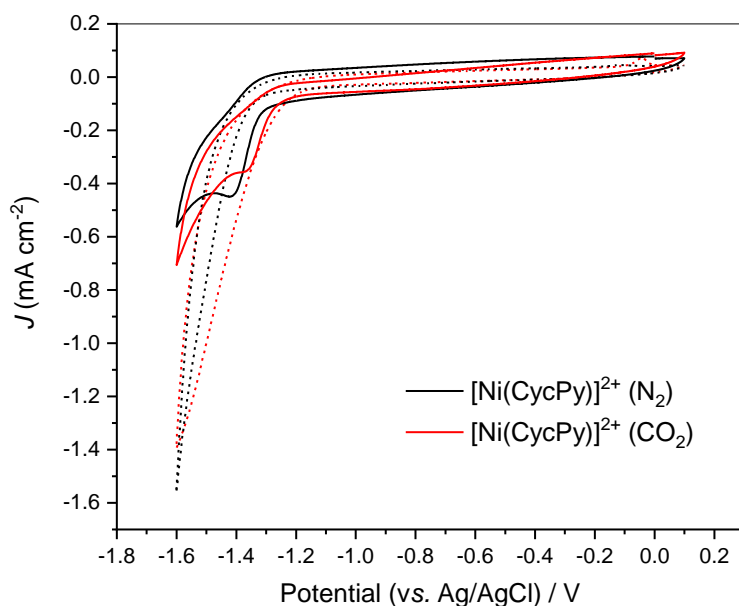


Figure 2 CVs of 1mM $[\text{Ni}(\text{CycPy})]^{2+}$ in 0.5M KHCO_3 at 100mV/s under N_2 (black) and CO_2 (red) using a GCE. The solvent window recorded under the same conditions in the absence of the catalysts is shown with dashed lines.

CVs in aqueous electrolyte (0.5 M KHCO_3) are shown in figure 2 for $[\text{Ni}(\text{CycPy})]^{2+}$ at a GCE. KHCO_3 was chosen as an electrolyte as it is commonly used in co-electrolysis with immobilised CO_2 reduction catalysts.^{29,30} In aqueous electrolyte the Ni^{III} reduction becomes irreversible suggesting that the Ni^{I} species is able to interact with the higher concentration of H^+ in the aqueous electrolyte, figure S5. The proximity of the solvent window to the Ni^{III} reduction peak makes it hard to distinguish if electrocatalytic CO_2 reduction occurs from CV analysis alone but under CO_2 the Ni^{III} reduction peak is shifted from -1.41 V (N_2) to -1.36 V (CO_2) demonstrating that CO_2 is still able to bind to the reduced (Ni^{I}) catalyst in aqueous solvents. One possible reason for the past lack of reports of electrocatalysis in water for immobilised Ni cyclam complexes is that loss of one N-H group inhibits catalysis and CO_2

binding.²⁶ Here we have carried out bulk electrolysis experiments using $[\text{Ni}(\text{CycPy})]^{2+}$ (0.2 mM) in 0.5 M KHCO_3 for 2 hours at -1.4 V with an average current density of 0.17 mA cm^{-2} and we find that CO and H_2 are the sole reaction products formed in a 1:1 ratio (CO: H_2 , total Faradic Efficiency 92%, Table S1). The selectivity is decreased when compared to the 4.5:1 reported for $[\text{Ni}(\text{Cyc})]^{2+}$ in a KCl electrolyte at a glassy carbon electrode²² but it still indicates that the addition of the pyrene group has not turned off CO_2 catalysis in water.

To test if the $[\text{Ni}(\text{CycPy})]^{2+}$ catalyst can form a non-covalent interaction with carbon supports we prepared electrodes by soaking glassy carbon plates in solutions of $[\text{Ni}(\text{CycPy})]^{2+}$ in methanol. The GCE plates were then washed with methanol followed by distilled water. X-ray photoelectron spectroscopy (XPS) of the $[\text{Ni}(\text{CycPy})]^{2+}$ powder shows a Ni $2p_{3/2}$ signal at 854.9 eV with broad satellite peaks (857-861 eV) due to the Ni^{2+} , with the binding energy being in very good agreement with the previous reported spectrum of $[\text{Ni}(\text{Cyc})]^{2+}$, figure S7.³⁴ The XPS spectrum of the as prepared GCE/ $[\text{Ni}(\text{CycPy})]$ electrode shows a Ni $2p_{3/2}$ signal at 856.2 eV. A previously reported Ni cyclam modified with pyrene on carbon nanotubes had a Ni^{2+} $2p_{3/2}$ binding energy of 856.0 eV.³¹ The shift to higher binding energies of the Ni $2p_{3/2}$ peaks upon immobilisation suggest an electron density shift away from the Ni centre to the carbon support upon immobilisation. The presence of the cyclam ligand is also confirmed through the observation of the N 1s signal at 400.3 eV (figure S6) confirming the successful immobilisation of the Ni cyclam pyrene complex on the GCE. Control XPS experiments where the $[\text{Ni}(\text{CycPy})]^{2+}$ was replaced with NiCl_2 in the soaking solution showed that following washing no significant concentration of Ni was retained on the electrode surface, figure S7.

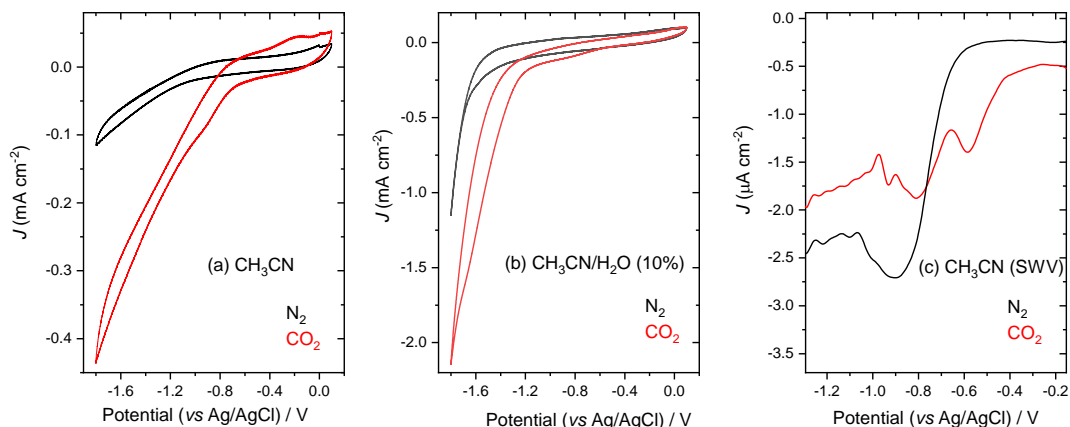


Figure 3 (a) CVs of GCE/[Ni(CycPy)] electrode in 0.1M TBA PF₆ in CH₃CN and (b) 0.1M TBA PF₆ in CH₃CN/H₂O (10%) at 100 mV/s under N₂ (black) and CO₂ (red). (c) SWV of GCE/[Ni(CycPy)] electrode in 0.1M TBA PF₆ in CH₃CN at 5Hz under N₂ (black) and CO₂ (red).

CVs of the GCE/[Ni(CycPy)] electrodes under N₂ and CO₂ (figure 3a) in CH₃CN show clear differences to an unmodified GCE (see solvent window in figure 1a) also confirming the presence of the catalyst. Under N₂ we find that the current density becomes increasingly negative at < -0.95 V. Square wave voltammetry (SWV, figure 3c) shows the presence of a reduction at -0.90 V which is proposed to be the Ni^{II/I} reduction of immobilised [Ni(CycPy)]²⁺ due its sensitivity to CO₂ (see below). From the electrochemical data (figures S8,9) we measure a surface coverage of 1.1 x 10⁻¹⁰ mol cm⁻² for [Ni(CycPy)]²⁺ on the glassy carbon electrode. This is similar to the surface coverage achieved by Kubiak and co-workers using an electrografting approach for cyclam complexes, where values of 1.3 x 10⁻¹⁰ to 2.3 x 10⁻¹⁰ mol cm⁻² were measured, which was calculated to be equivalent to monolayer coverages.²⁶ Assuming that the pyrene group is laid flat on the electrode surface, and that no other part of the complex is in-contact with the electrode surface, we estimate the theoretical maximum monolayer coverage to be 2.8 x 10⁻¹⁰ mol cm⁻², Figure S10. This is an estimated maximum

surface coverage as in reality the presence of the alkyl chain and cyclam group will increase the effective footprint of the catalyst on the surface. The measured value of 1.1×10^{-10} mol cm^{-2} for $[\text{Ni}(\text{CycPy})]^{2+}$ is on the order expected based on both this calculation and past experimental reports. Variable scan rate studies confirm that the reduction is due to a surface confined process, confirming its assignment to the $[\text{Ni}(\text{CycPy})]^{2+}$ complex and demonstrating that successful immobilisation of an electroactive species has occurred, figure S9.

The $\text{Ni}^{\text{II/I}}$ reduction is shifted *ca.* 450 mV positive upon immobilisation under N_2 demonstrating that the $[\text{Ni}(\text{CycPy})]^{2+}$ complex is interacting strongly with the carbon surface. This is supported by the XPS data which suggested a decrease in electron density at the Ni centre upon immobilisation. A similar shift in the reduction potential was observed by Fontecave and co-workers upon immobilisation of a modified Ni cyclam complex on a carbon nanotube electrode.³¹ The very large shift in reduction potential upon immobilisation therefore appears to be a common feature of this class of catalysts that requires further investigation. On mercury electrodes the $\text{Ni}^{\text{II/I}}$ couple is also shifted positive due to the reduced Ni^{I} state being stabilised through interaction with the metal surface and a beneficial effect on the onset of CO_2 catalysis occurs.¹³ Indeed here we find under CO_2 that the current density increases slightly at potentials negative of -0.8 V, with a larger increase in current density with applied potential negative of -1.1V. The increased current density at -0.8 V suggests that immobilisation offers a way to achieve a significant decrease in overpotential for catalysis. Although no proton source has been deliberately added in the experiment shown in figure 3a, residual water particularly after the CO_2 purge will be present. Addition of 10% water leads to a large increase in current density for CVs recorded under CO_2 using the GCE/ $[\text{Ni}(\text{CycPy})]$ electrode at potentials negative of -1.1 V when compared to the same electrode under CO_2 in CH_3CN alone, figure 3b. The oxidation at -0.2 V under CO_2 (figure 3 a) is similar to that seen for $[\text{Ni}(\text{Cyc})]^{2+}$ at carbon electrodes under similar conditions. This feature has been assigned to the oxidation of a $[\text{Ni}^0-$

carbonyl] complex formed by reduction of $[\text{Ni}(\text{Cyc})(\text{CO})]^+$.¹² CO is present in the experiments as it is formed through CO₂ reduction. SWV shows reductions at -0.58 V and at -0.81 V under CO₂. The reduction at -0.81 V is proposed to be due to the Ni^{III/I} reduction of $[\text{Ni}(\text{CycPy})]^{2+}$ which is accompanied by CO₂ binding, whilst the peak at -0.58 V is proposed to be due to the formation of a CO bound Ni^I complex.¹² The large binding constant of Ni^I cyclams towards CO (for $[\text{Ni}(\text{Cyc})]^+$ in CH₃CN, $K_{\text{CO}} = 2.8 \pm 0.6 \times 10^5 \text{ M}^{-1}$, $K_{\text{CO}_2} = 4 \pm 2 \text{ M}^{-1}$)^{33,35} means that even trace amounts can lead to large shifts in the Ni^{III/I} reduction potential.

Figure 3 indicates that the $[\text{Ni}(\text{CycPy})]^{2+}$ immobilised on a GCE electrode remains active towards CO₂ upon immobilisation. In aqueous KHCO₃ (0.5 M) the CVs of the immobilised complex show a large current increase under CO₂ at potentials negative of -1.1 V when compared to N₂ (figure S10) however no clear Ni^{III/I} reduction features could be observed. Attempts to carry out bulk electrolysis using the immobilised catalyst on a GCE gave H₂ as the dominant (>95% Faradic efficiency) product with a Faradic Efficiency of *ca.* 0.6% for CO, table S1. XPS post electrolysis demonstrates that the majority of the $[\text{Ni}(\text{CycPy})]^{2+}$ complex is lost from the electrode surface during bulk electrolysis, figure S7. These results show that the non-covalent interaction between the pyrene group and the carbon surface is insufficient to prevent desorption of the majority of the catalyst over prolonged periods at negative potentials, in solvents in which the complex readily dissolves.

Although the pyrene-carbon electrode interaction is insufficient alone to prevent desorption the electrochemical data in figure 3 indicates that the immobilisation offers an advantage through the modification of the Ni^{III/I} reduction potential. Although weak, the XPS of the post electrolysis sample also showed that the remaining Ni was in a similar form to the sample pre-electrolysis. Therefore we persisted and also tested $[\text{Ni}(\text{CycPy})]^{2+}$ on a gas diffusion electrode (GDE) support in a flow through structure. In a GDE structure the wetting of the catalyst layer is limited by the additional PTFE added to the catalyst ink used when preparing the electrode

which was hoped would improve the electrode stability. Furthermore the GDE structure allows for delivery of a high CO₂ concentration and removal of CO produced at the electrode which would help overcome CO poisoning, a known limitation of this class of catalysts.^{10,12,22,31} Experiments were carried out using a 0.5 M KHCO₃ catholyte flowed at 12 ml min⁻¹ and the CO₂ gas feed was delivered to the back of the GDE structure at 20 ml min⁻¹. In this preliminary report we describe the results for the GDE/[Ni(CycPy)] electrode held at -1.4 V versus a Ag/AgCl reference electrode that was present in the catholyte, figure 4. Additional experiments using a carbon filler in the catalyst ink to increase the current density of the GDE/[Ni(CycPy)] electrode are shown in figure S13. For the duration of the experiment CO was detected indicating that the [Ni(CycPy)]²⁺ electrode is able to electrocatalytically reduce CO₂ when immobilised on the GDE support using an aqueous catholyte. The initial turnover frequency of the catalyst is calculated to be ~55 hr⁻¹ based off the measured catalyst concentration on the electrode surface, figure S12a. The first reports of the use of molecular electrocatalysts on GDE structures have only been made recently and to date these have focussed on the Fe and Co macrocyclic complexes, particularly porphyrins.³⁶⁻³⁸ The only previous studies on GDE supports using Ni cyclam catalysts that we are aware of have used non-aqueous electrolytes.^{31,39} The finding here that we can produce CO using a [Ni(CycPy)]²⁺ GDE in 0.5 M KHCO₃ suggests that this class of catalysts has potential for use in complete aqueous electrolyzers. We do find that both the current and selectivity towards CO₂ decreases over 140 minutes of use with increased levels of H₂ production occurring at longer times. From figure S12(b) we see that even with the PTFE present in the catalyst ink NiCycPy is still lost from the GDL into the solution, demonstrating that catalyst loss from the surface, not poisoning, is the primary cause of the loss of selectivity to CO production. The catalyst loss from the surface also highlights an important wider issue for the electrochemistry community. π - π stacking of pyrene groups on carbon supports is widely used as a simple way to non-covalently modify

electrodes in the sensing and catalysis communities, particularly for CO₂ reduction,^{27,28,30,40} but desorption is not commonly discussed. Here, we find that although stable at open circuit conditions under an applied bias the pyrene modified species desorbs. A study on 1-pyrenecarboxylic acid on graphite showed that at potentials negative of the pyrene reduction potential (-0.8 V), desorption began to occur over prolonged periods, in-line with our observation of slow catalyst loss from the GDE surface. Pyrene loss occurred at low levels at near neutral pH's but at high pH's the pyrene group was completely removed.⁴¹ This is important as during CO₂ reduction experiments, such as those reported here, potentials significantly negative of -0.8 V (vs. Ag/AgCl) are typically applied and the local pH in GDE's is known to rise due to H⁺ consumption via H₂O dissociation to pH >12.⁴² It is clear that the pyrene group can play an important role in controlling the orientation of interaction of the catalyst with the electrode surface, and in facilitating electron transfer, and here its presence leads to a +0.45 V shift in the Ni^{II/I} reduction potential, however in-itself it is insufficient to ensure stable immobilisation under catalytic conditions. Future experiments on [Ni(CycPy)]²⁺ GDE's will focus on both the formulation of the catalyst ink to increase and modification of the cyclam structure to reduce solubility in an effort to further increase the electrode stability. More widely we propose that the community should also be focused on additional catalyst modifications to decrease the solubility of the catalyst in aqueous solvents to prevent desorption.

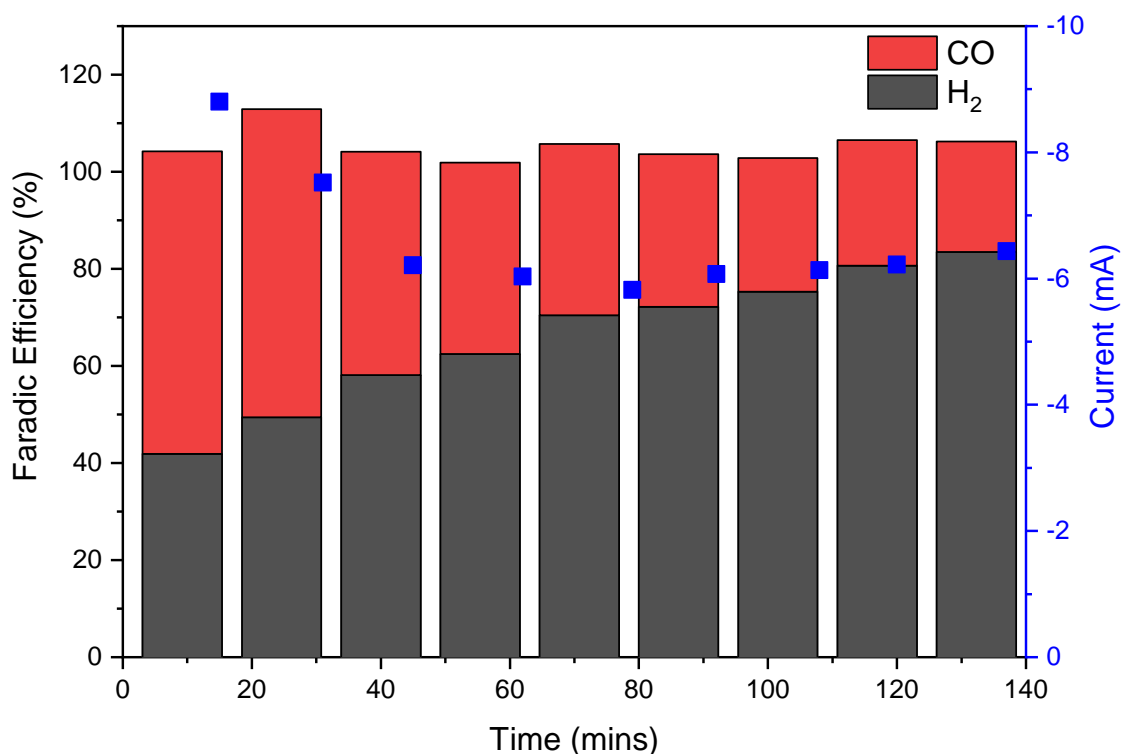


Figure 4. Electrolysis data from a $[\text{Ni}(\text{CycPy})]^{2+}$ GDE used in 0.5 M KHCO_3 with a CO_2 flow rate of 20 ml min^{-1} .

Conclusions A new, previously unreported, pyrene modified Ni cyclam complex ($[\text{Ni}(\text{Cyc-Py})]^{2+}$) has been synthesised and electrochemically characterised. In both aqueous and mixed solvents ($\text{CH}_3\text{CN}/\text{H}_2\text{O}$ (10%)) $[\text{Ni}(\text{Cyc-Py})]^{2+}$ shows similar behaviour to the parent $[\text{Ni}(\text{Cyc})]^{2+}$ complex and is an active catalyst for CO_2 reduction, although selectivity towards CO_2 is slightly decreased. The decreased selectivity is likely due to the loss of one of the 4 N-H groups on the cyclam ligand which are known to aid CO_2 binding.^{17,26,33,43}

XPS and electrochemical measurements show that the pyrene group enables immobilisation onto a carbon surface. Although the strength of the non-covalent π - π interaction is insufficient to prevent the complex from desorbing in an aqueous solvent upon application of a reducing

potential it is shown from experiments in mixed solvents that immobilisation leads to a large (+0.45 V) positive shift in the potential of the Ni^{II/I} reduction. In a GDE set-up the stability of the immobilised [Ni(CycPy)]²⁺ electrode is increased and preliminary studies using an aqueous electrolyte are possible. This is important as past studies using immobilised cyclams had focussed on mixed solvents. Here we provide the first report using an immobilised cyclam complex on a GDE support in aqueous electrolyte that shows that CO production does occur, furthermore our studies indicate that activity is decreasing not because of catalyst poisoning but due to catalyst loss from the surface. Therefore, there is no fundamental reason why Ni cyclams cannot operate in a practical CO₂ electrolyser. We propose that [Ni(CycPy)]²⁺ is a promising catalyst for future development and future studies should focus on the engineering of the GDE structure to increase current densities and to increase device stability.

Acknowledgements This work is supported by UKRI-EPSC funding (EP/P034497/1, EP/N010531/1). We also thank the University of Liverpool for support of a studentship (FG) and access to funding through the Partnership Recovery and Resilience Fund. The x-ray photoelectron (XPS) data collection was performed at the EPSC National Facility for XPS (“HarwellXPS”), operated by Cardiff University and UCL, under Contract No. PR16195.

References

- 1 E. E. Benson, C. P. Kubiak, A. J. Sathrum and J. M. Smieja, *Chem. Soc. Rev.*, 2009, **38**, 89–99.
- 2 J. Qiao, Y. Liu, F. Hong and J. Zhang, *Chem Soc Rev*, 2014, **43**, 631–675.

- 3 H. Takeda, C. Cometto, O. Ishitani and M. Robert, *ACS Catal.*, 2017, **7**, 70–88.
- 4 Y. Hori, *Mod. Asp. Electrochem.*, 2008, **42**, 89–189.
- 5 L. Sun, V. Reddu, A. C. Fisher and X. Wang, *Energy Environ. Sci.*, 2020, **13**, 374–403.
- 6 B. Fischer and R. Eisenberg, *J. Am. Chem. Soc.*, 1980, **102**, 7361–7363.
- 7 M. Beley, J. Collin, R. Ruppert and J. Sauvage, *J. Chem. Soc., Chem. Commun.*, 1984, **2**, 1315–1316.
- 8 J. P. Collin, A. Jouaiti and J. P. Sauvage, *Inorg. Chem.*, 1988, **27**, 1986–1990.
- 9 M. Beley, J. P. Collin, R. Ruppert and J. P. Sauvage, *J. Am. Chem. Soc.*, 1986, **108**, 7461–7467.
- 10 S. L. Behnke, A. C. Manesis and H. S. Shafaat, *Dalt. Trans.*, 2018, **47**, 15206–15216.
- 11 J. Song, E. L. Klein, F. Neese and S. Ye, *Inorg. Chem.*, 2014, **53**, 7500–7507.
- 12 J. D. Froehlich and C. P. Kubiak, *J. Am. Chem. Soc.*, 2015, **137**, 3565–3573.
- 13 C. A. Kelly, E. L. Blinn, N. Camaioni, M. D’Angelantonio and Q. G. Mulazzani, *Inorg. Chem.*, 1999, **38**, 1579–1584.
- 14 C. A. Kelly, Q. G. Mulazzani, E. L. Blinn and M. A. J. Rodgers, *Inorg. Chem.*, 1996, **35**, 5122–5126.
- 15 M. Fujihira, Y. Hirata and K. Suga, *J. Electroanal. Chem.*, 1990, **292**, 199–215.
- 16 K. Bujno, R. Bilewicz, L. Siegfried and T. A. Kaden, *J. Electroanal. Chem.*, 1998, **445**, 47–53.
- 17 A. Jarzebinska, P. Rowinski, I. Zawisza, R. Bilewicz, L. Siegfried and T. Kaden,

- Anal. Chim. Acta*, 1999, **396**, 1–12.
- 18 Y. Wu, B. Rudsheteyn, A. Zhanaidarova, J. D. Froehlich, W. Ding, C. P. Kubiak and V. S. Batista, *ACS Catal.*, 2017, **7**, 5282–5288.
- 19 J. Billo and P. J. Connolly, *Inorg. Chem.*, 1987, **26**, 3224–3226.
- 20 J. Schneider, H. Jia, K. Kobiro, D. E. Cabelli, J. T. Muckerman and E. Fujita, *Energy Environ. Sci.*, 2012, **5**, 9502–9510.
- 21 G. Neri, I. M. Aldous, J. J. Walsh, L. J. Hardwick and A. J. Cowan, *Chem. Sci.*, 2016, **7**, 1521–1526.
- 22 J. D. Froehlich and C. P. Kubiak, *Inorg. Chem.*, 2012, **51**, 3932–3934.
- 23 G. Neri, J. J. Walsh, C. Wilson, A. Reynal, J. Y. C. Lim and A. J. Cowan, *Phys. Chem. Chem. Phys.*, 2015, **17**, 1562–1566.
- 24 Y. J. Leem, K. Cho, K. H. Oh, S. Han, K. M. Nam and J. Chang, *Chem Soc Rev*, 2017, **53**, 3454–3457.
- 25 C. R. Schneider and H. S. Shafaat, *Chem. Commun.*, 2016, **52**, 9889–9892.
- 26 A. Zhanaidarova, C. E. Moore, M. Gembicky and C. P. Kubiak, *Chem. Commun.*, 2018, **54**, 4116–4119.
- 27 J. D. Blakemore, A. Gupta, J. J. Warren, B. S. Brunshwig and H. B. Gray, *J. Am. Chem. Soc.*, 2013, **135**, 18288–18291.
- 28 P. Kang, S. Zhang, T. J. Meyer and M. Brookhart, *Angew. Chemie Int. Ed.*, , DOI:10.1002/anie.201310722.
- 29 A. Maurin and M. Robert, *J. Am. Chem. Soc.*, 2016, **138**, 2492–2495.
- 30 B. Reuillard, K. H. Ly, T. E. Rosser, M. F. Kuehnel, I. Zebger and E. Reisner, *J. Am.*

- Chem. Soc.*, 2017, **139**, 14425–14435.
- 31 S. Pugliese, N. T. Huan, J. Forte, D. Grammatico, S. Zanna, B. Su, Y. Li and M. Fontecave, *ChemSusChem*, 2020, **13**, 6449–6456.
- 32 A. D. Cabral, B. I. Murcar-Evans, K. Toutah, M. Bancarz, D. Rosa, K. Yuen, T. B. Radu, M. Ali, A. Penkul, D. Kraskouskaya and P. T. Gunning, *Analyst*, 2017, **142**, 3922–3933.
- 33 D. J. Szalda, E. Fujita, R. Sanzenbacher, H. Paulus and H. Elias, *Inorg. Chem.*, 1994, **33**, 5855–5863.
- 34 S. P. Roe, J. O. Hill, J. Liesegang, S. P. Roe, J. O. Hill and J. Liesegang, *Transit. Met. Chem. IO*, 1985, 100–106.
- 35 M. Hammouche, D. Lexa, J. M. Savêant and M. Momenteau, *J. Am. Chem. Soc.*, 1991, **113**, 8455–8466.
- 36 K. Murata, H. Tanaka and K. Ishii, *J. Ph.*, 2019, **123**, 12073–12080.
- 37 S. Ren, D. Joulié, D. Salvatore, K. Torbensen, M. Wang, M. Robert and C. P. Berlinguette, *Science (80-.)*, 2019, **365**, 367–369.
- 38 K. Torbensen, D. Joulié, S. Ren, M. Wang, D. Salvatore, C. P. Berlinguette and M. Robert, *ACS Energy Lett.*, 2020, **5**, 1512–1518.
- 39 C. Jiang, A. W. Nichols, J. F. Walzer and C. W. Machan, *Inorg. Chem.*, 2020, **59**, 1883–1892.
- 40 L. A. Paul, Sheida Rajabi, Christian Jooss, Franc Meyer, Fatemeh Ebrahimi and Inke Siewert, *Dalt. Trans.*, 2020, **49**, 8367–8374.
- 41 M. Cao, A. Fu, Z. Wang, J. Liu, N. Kong, X. Zong, H. Liu and J. J. Gooding, *J. Phys.*

- Chem. C*, 2014, **118**, 2650–2659.
- 42 H. Rabiee, L. Ge, X. Zhang, S. Hu, M. Li and Z. Yuan, *Energy Environ. Sci.*, 2021, **14**, 1959–2008.
- 43 E. S. Rountree, B. D. Mccarthy, T. T. Eisenhart and J. L. Dempsey, *Inorg. Chem.*, 2014, **53**, 9983–10002.